JACC Vol. 30, No. 4
October 1997:1079–85

EXPERIMENTAL STUDIES

Reduced Sympathetic Innervation Underlies Adjacent Noninfarcted Region Dysfunction During Left Ventricular Remodeling

CHRISTOPHER M. KRAMER, MD, FACC, PHILIP D. NICOL, MD, WALTER J. ROGERS, MS, MARK M. SUZUKI, MD, AMY SHAFFER, BS, THERESE M. THEOBALD, RDCS, NATHANIEL REICHEK, MD, FACC

Pittsburgh, Pennsylvania

Objectives. **We examined the association of sympathetic denervation and reduced blood flow with mechanical dysfunction in adjacent noninfarcted regions late after myocardial infarction (MI).**

Background. **Using a well characterized ovine model of left ventricular (LV) remodeling after transmural anteroapical MI, we previously showed that histologically normal adjacent noninfarcted regions demonstrate mechanical dysfunction.**

Methods. **Ten sheep underwent coronary ligation. Magnetic resonance imaging was performed before and 8 weeks after infarction for measurement of LV mass, volumes, ejection fraction and regional intramyocardial circumferential shortening (%S). Iodine-123 metaiodobenzylguanidine (I-123 MIBG) and fluorescent microspheres before and after administration of adenosine were infused before death for measurement of sympathetic innervation, blood flow and blood flow reserve from matched postmortem regions.**

Results. **From baseline to 8 weeks after infarction, LV end-diastolic volume increased from (mean ± SD) 1.5 ± 0.3 to 2.6 ± 0.5 ml/kg ($p < 0.001$), and LV mass increased from 2.0 ± 0.3 to 2.6 ± 0.5 g/kg ($p = 0.001$). Regionally, the decline in subendocardial %S was greater in adjacent (19 ± 5% to 8 ± 5%) than in remote noninfarcted regions (20 ± 6% to 19 ± 6%, $p < 0.002$). No difference in regional blood flow or blood flow reserve was found between adjacent and remote regions, whereas I-123 MIBG uptake was lower in adjacent than in remote myocardium (1.09 ± 0.30 vs. 1.31 ± 0.40 nmol/g, $p < 0.003$). Topographically, from apex to base at 8 weeks after infarction, %S correlated closely with I-123 MIBG uptake ($r = 0.93$, $p = 0.003$).**

Conclusions. **In mechanically dysfunctional noninfarcted regions adjacent to chronic transmural myocardial infarction in the remodeled left ventricle, blood flow and blood flow reserve are preserved, yet sympathetic innervation is reduced. Chronic sympathetic denervation in adjacent noninfarcted regions, in association with regional mechanical dysfunction, may contribute to LV remodeling after infarction.**

(J Am Coll Cardiol 1997;30:1079–85

Late after transmural anteroapical myocardial infarction (MI), histologically normal adjacent noninfarcted regions are mechanically dysfunctional (1,2). Function in adjacent regions improves somewhat between 1 and 8 weeks after infarction but remains depressed relative to remote noninfarcted regions to 6 months after MI (1). Potential mechanisms for this dysfunction include increased local wall stress (3), altered sympathetic nervous function (4), reduced coronary blood flow (5), excess cellular hypertrophy (2,6) and intrinsic myocyte dysfunction (2).

Metaiodobenzylguanidine (MIBG) is an analogue of norepinephrine and guanethidine that is taken up by sympathetic nerve terminals and can be labeled with iodine-123 (I-123) for purposes of imaging or quantitation in myocardium and other tissues (7–9). We used magnetic resonance myocardial tagging (10–12) to measure mechanical function, MIBG uptake to assess sympathetic innervation and fluorescent microspheres (13) to measure myocardial blood flow on a topographic and regional basis in the remodeled ovine left ventricle 8 weeks after anteroapical infarction. We hypothesized that sympathetic innervation could be quantified and matched to blood flow and mechanical function in the remodeled left ventricle and that denervation or reduced blood flow, or both, might contribute to mechanical dysfunction.

Methods

Coronary ligation. In 10 Q fever–negative female Dorsett sheep, a left thoracotomy was performed as previously described (1,14), with ligation of the left anterior descending coronary artery and its second diagonal branch to create a moderate-sized anteroapical infarction. Three additional control animals did not undergo infarction. All procedures were in accordance with the "Position of the American Heart Associ-

From the Division of Cardiology, Department of Medicine, Allegheny University of the Health Sciences, Allegheny General Hospital, Pittsburgh, Pennsylvania. This study was supported by a grant-in-aid from the American Heart Association, Pennsylvania affiliate and by a grant from the Allegheny University of the Health Sciences, Pittsburgh, Pennsylvania.

Manuscript received February 3, 1997; revised manuscript received May 13, 1997, accepted June 21, 1997.

Address for correspondence: Dr. Christopher M. Kramer, Cardiology Division, Allegheny General Hospital, 320 East North Avenue, Pittsburgh, Pennsylvania 15212. E-mail: ckramer@pgh.auhs.edu.

Published by Elsevier Science Inc.

0735-1097/97/$17.00
PII S0735-1097(97)00244-1

Abbreviations and Acronyms

ANOVA = analysis of variance
ECG = electrocardiographic
I-123 = iodine-123
LV = left ventricular
MI = myocardial infarction
MIBG = metaiodobenzylguanidine
MRI = magnetic resonance imaging
%S = regional percent intramyocardial circumferential segment shortening
TE = echo time
TR = repetition time

ation on Research Animal Use," adopted by the Association in November 1984, and the Institutional Animal Care and Use Committee at Allegheny University of the Health Sciences, Allegheny Campus.

Magnetic resonance imaging. The 10 infarcted sheep underwent magnetic resonance imaging (MRI) on a Siemens 1.5-tesla Magnetom at baseline, before the coronary ligation and again 8 weeks after infarction. The three control animals underwent one MRI session. Before the imaging sessions, all animals were premedicated intravenously with diazepam (1 mg), penicillin (22,000 U/kg) and gentamicin (3 mg/kg body weight). Intravenous 5% guaifenesin and 500 mg of ketamine provided heavy sedation during imaging. Intubation, mechanical ventilation, nasogastric suction and electrocardiographic (ECG) monitoring were performed. The animal was placed in the right lateral decubitus position and ECG gating was initiated.

After scout images were obtained, the timing of end-systole was identified as the point of minimal (left ventricular) LV cavity area by a multiphase, single-slice, short-axis cine series at the base of the ventricle, with frames obtained at 40-ms intervals. A breath-hold, multiple phase-encoded, gradient echo sequence with segmented k-space sampling (15,16) was used for evaluation of regional function. A contiguous series of multiphase, single-slice, 7-mm thick, tagged images spanning the left ventricle from base to apex was performed (Fig. 1). Imaging variables included an interstripe distance of 7 mm, a repetition time (TR) of 8 ms, an echo time (TE) of 1 to 5 ms, a 126 × 256 matrix and a 28-cm field of view, yielding a final interpolated pixel size of 1.19 mm^2. Frame duration was adjusted between 58 to 80 ms in order to center one of the five frames at end-systole. The ventilator was held at end-expiration for 18 heartbeats to complete the breath-hold sequence.

For assessment of LV volumes and mass, a contiguous series of nontagged gradient echo images in the same planes as the tagged images was obtained. This sequence was a breath-hold (14 heartbeats), three-phase (end-diastole, mid-systole and end-systole), segmented k-space series of 7-mm thick images with a TR of 9 ms and a TE of 6 ms. The interpolated pixel size was 1.37 mm^2 based on a 126 × 256 matrix and a 30-cm field of view.

Figure 1. Short-axis, tagged magnetic resonance spin-echo image at the apex in the ovine model. Thinned, transmurally infarcted anteroseptal myocardium is seen from the 1 o'clock to 5 o'clock position in the image. Noninfarcted myocardium with normal transmural thickness within 2 cm of the infarction is termed adjacent.

MIBG labeling. Solid-phase labeling of MIBG with I-123 (Nordion International) was performed according to the methods of Washburn et al. (17). Two milligrams of MIBG (courtesy of Dr. D. Wieland, University of Michigan) was dissolved in 0.5 ml of distilled water and added to a rubber-stoppered, vented reaction vial containing 10 mg of ammonium sulfate. The reaction was begun by adding 1 mCi of carrier-free I-123. The reaction vial was placed in an aluminum block heater at 165°C, and after complete evaporation of all water, incubation was continued for 1 h. I-123 MIBG was resuspended in 3 ml of water and a 2-ml aliquot was spotted onto a thin layer chromatography plate, then radiopharmaceutical purity was determined by chromatography in ammonium hydroxide/ethyl acetate/ethanol (1:20:20). Radiochemical purity of I-123 MIBG by this method was 96.3 ± 0.4%. Specific activity of MIBG was determined by counting incorporation of ^{123}I into MIBG in a Packard Minaxi Autogamma 5000 counter. No separation of free from bound iodine was performed before injection of I-123 into the animals. Blood pool activity was expressed in counts per gram of whole blood.

I-123 MIBG uptake and microsphere blood flow. At 8 weeks after infarction, after the MRI session, the thorax was opened and the left atrium and descending aorta were cannulated. All animals were injected with 3 million, 15-mm, fluorescent latex microspheres (13) through the left atrium before adenosine infusion (0.1 μg/kg per min) and then injected with the same volume of microspheres of a different fluorescence

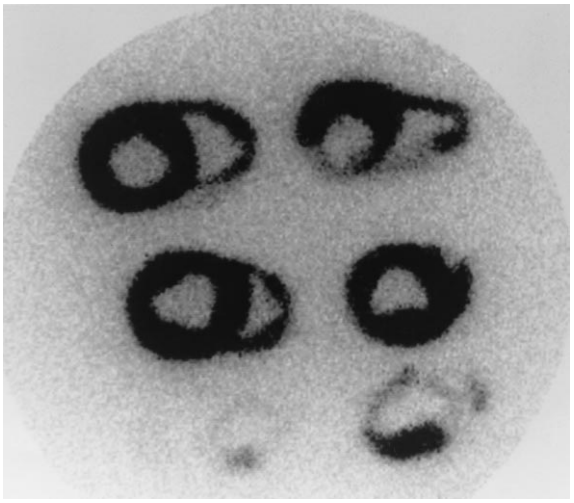

Figure 2. Image of I-123 MIBG uptake of 1-cm thick slices of a postmortem ovine heart taken on a gamma camera with a low energy, all-purpose collimator. Note the grossly reduced I-123 MIBG uptake in infarcted regions in the three slices at **bottom** and in the aortic and pulmonic valve planes in the slice at **upper right**. These slices were then sectioned further for quantitative assessment of I-123 MIBG uptake.

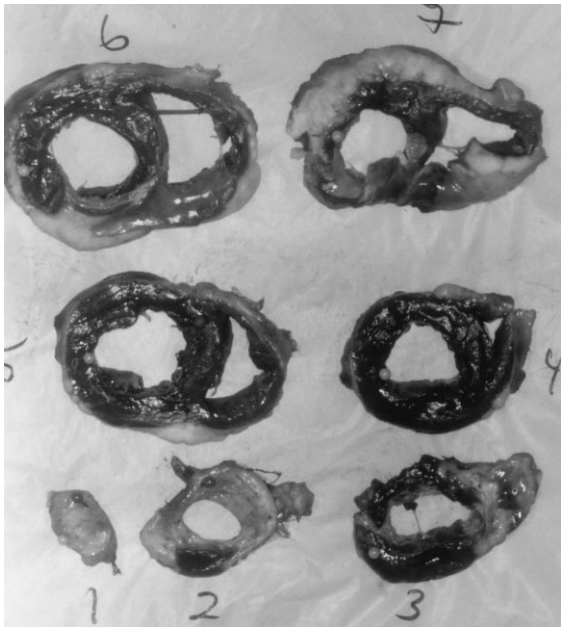

Figure 3. Photograph of slices from the same heart as that in Figure 2. Slice numbers and orientation correspond exactly with those in Figure 2 from slice 1 (apex) to slice 7 (base). Note that slice 1 and most of slice 2 are replaced with thinned, fat-infiltrated infarcted tissue. Slice 3 corresponds to the image in Figure 1 with transmurally infarcted tissue in the anteroseptum (from 1 o'clock to 5 o'clock).

during the infusion. Blood samples were withdrawn for a total of 3 min (1 min before and 1.5 min after a 30-s injection of microspheres) at a constant rate (5 ml/min) from the descending aorta for control measurement of fluorescence.

All animals were then injected with 1.4 ± 0.1 mCi of I-123 MIBG. After 60 min, the heart was excised, cut into 1-cm thick slices and imaged on a GE Starcam 300 equipped with a low energy all-purpose (LEAP) collimator (Fig. 2). A 20% window at 159 keV with a 256 × 256 matrix was used for imaging. A total of 500,000 counts was obtained for each set of slices. The slices were then photographed in the same orientation (Fig. 3). The sharply defined infarct borders were identified, and tissue within 2 cm of the transmural infarct was termed adjacent, whereas tissue beyond 2 cm was termed remote, as previously defined (1,16). The slices were further sectioned into 1- to 2-g samples for counting. The MIBG myocardial uptake was expressed in counts per gram, and using the specific activity, absolute molar MIBG uptake was determined for each piece. Molar uptake of MIBG per gram of tissue was then compared by slice from apex to base (Fig. 2 and 3) and by the noninfarct-related region.

Infarcted tissue was weighed and percent infarct was calculated as infarct weight/total LV weight. Data from control animals were analyzed by slice and by region along the long axis of the ventricle (apex, mid and base).

For quantitation of regional myocardial blood flow, the same 1- to 2-g pieces of myocardium were digested in 10 mL of 4 mol/liter KOH and 2% Tween 80 over 48 h. The digested tissue was filtered and washed to recover residual microspheres, and the fluorescent dyes were released using 1.25 ml of Cellosolve acetate for 24 h. The fluorescence of the samples before and during adenosine infusion was determined by using an automated fluorescence spectrophotometer (Perkin-Elmer LS-50B) and compared with that of reference blood samples prepared in the same manner. Blood flow from tissue samples before and during adenosine infusion as a measure of flow reserve was compared in adjacent and remote noninfarcted regions. Data from control animals were analyzed by apex to base location.

Magnetic resonance image analysis. Images were transferred to a SUN workstation for analysis. LV mass, end-diastolic and end-systolic volumes and ejection fraction were measured by a single investigator (T.M.T.) from nontagged gradient echo images using Siemens Imageview software (Siemens Corporate Research) and published techniques (1,16). Regional percent intramyocardial circumferential segment shortening (%S) was assessed using a software package (VIDA, University of Iowa) that allows measurement of interstripe distances within the myocardium along operator-placed lines displaying pixel amplitude values (1,12,16). Interstripe distances were measured at end-systole (L_{es}) and end-diastole (L_{ed}). Percent S was calculated as $\%S = 100(L_{ed}-L_{es})/L_{ed}$ and was measured at endocardial and epicardial sites in segments in each imaged slice from apex to base and also by region (adjacent and remote), as defined earlier and as previously described (1,16). Data from control animals were analyzed by apex to base location.

Statistical analysis. Results are displayed as mean value ± SD. Changes in global variables of remodeling from baseline to 8 weeks after infarction in the animals were assessed by the Student paired *t* test. Regional changes in %S between base-

Table 1. Percent Intramyocardial Circumferential Shortening, Iodine-123 Metaiodobenzylguanidine Uptake, Myocardial Blood Flow and Blood Flow Reserve by Level in Control Animals*

Level	%S	I-123 MIBG Uptake (nmol/g)	Blood Flow (ml/g per min)	Blood Flow Reserve
1 (apex)	17 ± 1%	1.46 ± 0.40	0.82 ± 0.16	2.2 ± 1.7
2	17 ± 1%	1.46 ± 0.33	0.94 ± 0.27	2.4 ± 1.6
3	17 ± 4%	1.48 ± 0.54	0.87 ± 0.28	2.4 ± 1.8
4	17 ± 1%	1.40 ± 0.67	0.86 ± 0.29	2.3 ± 1.7
5	18 ± 1%	1.47 ± 0.46	0.99 ± 0.29	2.4 ± 1.6
6 (base)	16 ± 2%	1.45 ± 0.38	0.90 ± 0.33	2.2 ± 1.3

*p = NS, by analysis of variance, for all comparisons. Data presented are mean value ± SD. I-123 = iodine-123; MIBG = metaiodobenzylguanidine; %S = regional percent intramyocardial circumferential segment shortening.

line and 8 weeks after infarction were assessed by two-way repeated measures analysis of variance (ANOVA) with Scheffé subtesting. Regional differences between the groups in myocardial blood flow and %S at 8 weeks after infarction were tested by two-way ANOVA with Scheffé subtesting. Variation in the absolute amount of I-123 MIBG infused per experiment precluded intergroup comparisons of I-123 MIBG uptake. Intragroup ANOVA with Scheffé subtesting was performed for regional I-123 MIBG uptake. I-123 MIBG uptake and %S by apex to base location in the postinfarct animals were compared by the Pearson product-moment correlation coefficient.

Results

Topographic relation of %S, I-123 MIBG uptake and blood flow in control animals. In the three control animals, mean regional MIBG uptake was 1.48 ± 0.38 nmol/g and mean blood flow and blood flow reserve were 0.91 ± 0.27 ml/g per min and 2.7 ± 1.6, respectively. No apex to base gradient was seen in these variables or in %S (Table 1). Endocardial/epicardial blood flow ratios were 1.2 ± 0.1 throughout the heart.

Global LV remodeling in postinfarct animals. From baseline to 8 weeks after infarction, end-diastolic volume increased from 1.5 ± 0.03 to 2.6 ± 0.5 ml/kg ($p < 0.001$), and end-systolic volume increased from 0.8 ± 0.3 to 1.8 ± 0.5 ml/kg ($p < 0.0001$). Ejection fraction fell from 47 ± 6% to 29 ± 3% ($p < 0.0001$), and LV mass increased from 2.0 ± 0.3 to 2.6 ± 0.5 g/kg ($p = 0.001$). Mean infarct mass as percent total LV mass on pathologic study at 8 weeks after MI was 15 ± 4%.

Topographic relation of %S, I-123 MIBG uptake and blood flow in postinfarct animals. The seven slices from apex to base (Fig. 2 and 3) were analyzed on a topographic basis for %S, I-123 MIBG uptake, blood flow and blood flow reserve (Table 2). Slices 1 and 2 mostly included infarcted tissue (Fig. 2 and 3) and showed reductions in all variables. Slice 3 contained predominantly adjacent tissue and demonstrated depressed %S and I-123 MIBG uptake, but preserved blood flow and blood flow reserve relative to basal slices. In slice 4, only %S was decreased relative to the base. Slices 6 and 7 contained remote noninfarcted myocardium. Topographically, %S and I-123 MIBG uptake paralleled each other closely (correlation factor 0.93, $p = 0.003$) (Fig. 4). I-123 MIBG uptake in slices 3 through 5 tended to be higher than %S relative to basal slices 6 and 7, suggesting that the extent of denervation in slices 3 through 5 may be greater than the extent of dysfunction.

Regional %S, I-123 MIBG uptake and blood flow in postinfarct animals. When the data were analyzed by noninfarcted region, as defined by proximity to the sharply demarcated infarct border, no significant change in %S from baseline to 8 weeks after MI was found in remote noninfarcted regions (20 ± 6% to 19 ± 6% in the subendocardium and 16 ± 3% to 16 ± 5% in the subepicardium), whereas in adjacent noninfarcted regions, %S fell from 19 ± 5% at baseline to 8 ± 5% in the subendocardium at 8 weeks after MI ($p < 0.002$) and from 14 ± 4% to 6 ± 4% in the subepicardium ($p < 0.004$).

Results of the regional analysis of intramyocardial blood flow, blood flow reserve and I-123 MIBG uptake in the three control animals and 10 postinfarct animals are presented in Table 3. No differences in any of these variables were seen between the mid and basal left ventricle in the control animals. In the postinfarct animals, no differences in regional blood flow or blood flow reserve were found between adjacent and remote noninfarcted regions. Mean blood flow was 1.53 ± 0.45 ml/g per min in adjacent regions and 1.48 ± 0.47 ml/g per min in remote regions—greater than the equivalent levels in control

Table 2. Percent Intramyocardial Circumferential Shortening, Iodine-123 Metaiodobenzylguanidine Uptake, Myocardial Blood Flow and Blood Flow Reserve by Level in Animals After Infarction

Level	%S	I-123 MIBG Uptake (nmol/g)	Blood Flow (ml/g per min)	Blood Flow Reserve
1 (apex)	1 ± 5*†‡§	0.27 ± 0.20*†‡§	0.48 ± 0.44*†‡§	0.7 ± 0.7*†‡§
2	7 ± 4*†‡	0.50 ± 0.36*†‡§	0.76 ± 0.37*†‡§	1.5 ± 0.9*†‡§
3	10 ± 6†	0.86 ± 0.51†	1.30 ± 0.51	2.9 ± 1.0
4	12 ± 8†	1.17 ± 0.67	1.48 ± 0.40	3.6 ± 0.8
5	16 ± 5	1.32 ± 0.78	1.49 ± 0.51	3.5 ± 0.8
6	18 ± 6	1.36 ± 0.75	1.38 ± 0.41	3.3 ± 0.7
7 (base)	16 ± 6	1.27 ± 0.67	1.38 ± 0.59	3.2 ± 0.9
p value (ANOVA)	<0.0001	<0.003	0.0001	<0.0001

By Scheffé subtesting, *$p < 0.05$ versus level 7. †$p < 0.05$ versus level 6. ‡$p < 0.05$ versus level 5. §$p < 0.05$ versus level 4. Data presented are mean value ± SD. ANOVA = analysis of variance; other abbreviations as in Table 1.

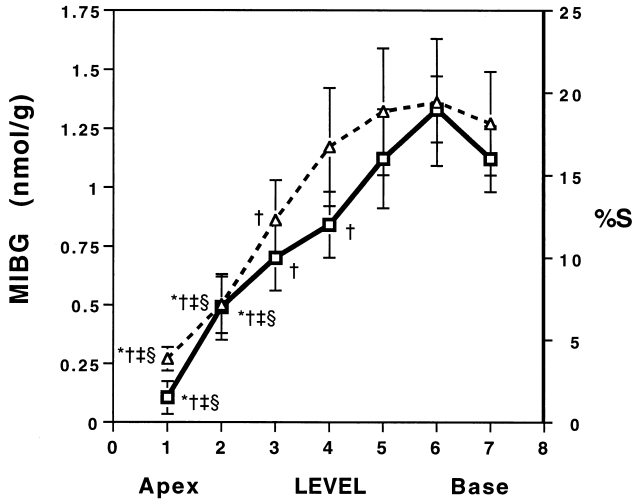

Figure 4. Graph of mean (±SD) MIBG uptake **(triangles)** on the leftward **y axis** and mean (±SD) %S **(squares)** on the rightward **y axis** based on apex to base slice location from the most apical slice 1 to the most basal slice 7. Slice locations are the same as those in Figures 2 and 3 and Table 2. $p < 0.0001$ for %S and $p < 0.003$ for I-123 MIBG uptake by ANOVA. By Scheffé subtesting, *$p < 0.05$ compared with level 7. †$p < 0.05$ compared with level 6. ‡$p < 0.05$ compared with level 5. §$p < 0.05$ compared with level 4. Slices 1 and 2 contain predominantly infarcted tissue, whereas slices 3 and 4 include some infarcted and some adjacent tissue, and slices 6 and 7 represent remote noninfarcted tissue. %S and I-123 MIBG uptake parallel each other closely (correlation factor 0.93, $p = 0.003$), implying a close match between sympathetic innervation and function at 8 weeks after infarction. I-123 MIBG uptake in slices 3 to 5 tends to be closer to the levels at the base of the heart than does %S, suggesting that the extent of denervation in these regions is greater than the extent of dysfunction.

Table 3. Regional Myocardial Blood Flow, Blood Flow Reserve and Iodine-123 Metaiodobenzylguanidine Uptake in Control and Animals After Infarction

	Control Animals		Postinfarction Animals	
	Mid	Base	Adjacent	Remote
Blood flow (ml/g per min)				
Endo	0.93 ± 0.30	1.07 ± 0.33	1.68 ± 0.49*	1.52 ± 0.53*
Epi	0.80 ± 0.27	0.88 ± 0.26	1.41 ± 0.41*	1.39 ± 0.58*
Endo/epi	1.2 ± 0.1	1.2 ± 0.1	1.2 ± 0.1	1.1 ± 0.2
Average	0.87 ± 0.28	0.97 ± 0.30	1.53 ± 0.45*	1.48 ± 0.47*
Blood flow reserve				
Endo	2.7 ± 1.6	2.5 ± 1.5	2.6 ± 1.3	2.8 ± 1.4
Epi	3.0 ± 2.0	2.8 ± 1.8	2.6 ± 1.0	2.8 ± 1.0
Average	2.8 ± 1.7	2.7 ± 1.5	2.6 ± 1.2	2.7 ± 1.0
I-123 MIBG uptake (nmol/g)				
Endo	1.51 ± 0.40	1.48 ± 0.38	1.08 ± 0.29†	1.32 ± 0.40
Epi	1.44 ± 0.33	1.46 ± 0.45	1.09 ± 0.31†	1.31 ± 0.40
Average	1.47 ± 0.35	1.47 ± 0.41	1.09 ± 0.30†	1.31 ± 0.40

*$p < 0.01$ versus control animals. †$p < 0.008$ versus remote region. Data presented are mean value ± SD. Endo = endocardial; Epi = epicardial; I-123 MIBG = iodine-123 metaiodobenzylguanidine.

animals. Endocardial/epicardial blood flow ratios were not different on a regional basis. Likewise, blood flow reserve was 2.6 ± 1.2 in adjacent regions and 2.7 ± 1.0 in remote regions, similar to control values. However, I-123 MIBG uptake was less in adjacent than in remote myocardium (1.09 ± 0.30 vs. 1.31 ± 0.40 nmol/g, $p < 0.003$). No differences between subendocardial and subepicardial blood flow reserve or I-123 MIBG uptake were found (Table 3).

Discussion

Using magnetic resonance tagging, we previously demonstrated that unscarred myocardium adjacent to transmural infarction in the ovine model is chronically dysfunctional as LV remodeling progresses (1). The present study shows that myocardial blood flow is increased relative to control levels in both adjacent and remote regions after infarction and that flow reserve is preserved, indicating that altered perfusion does not account for this dysfunction. However, sympathetic innervation is reduced in adjacent noninfarcted regions relative to remote regions that were matched for quantification of blood flow, I-123 MIBG uptake and mechanical function. Sympathetic denervation may contribute to the mechanical dysfunction found in adjacent noninfarcted regions, although the extent of denervation tended to be less than the extent of dysfunction.

Mechanisms of dysfunction. The present study demonstrates that blood flow and blood flow reserve are not reduced in adjacent noninfarcted regions 8 weeks after infarction. Therefore, neither rest ischemia nor repetitive stunning can account for the mechanical dysfunction in adjacent regions. Sympathetic denervation may account for part of the decline in function. Other postulated mechanisms for the dysfunction in adjacent regions include increased local wall stress (1,3) leading to excess cellular hypertrophy (2,6) and intrinsic myocyte dysfunction (2).

Sympathetic denervation after infarction. Early after infarction, Barber et al. (4) previously showed sympathetic denervation in adjacent noninfarcted regions. These investigators demonstrated that a transmural infarction in the dog produced acute sympathetic denervation in noninfarcted sites apical to the necrotic regions as measured by norepinephrine content and response to stellate stimulation, which recovered in part by 7 to 21 days after infarction. Kozlovskis et al. (18) similarly found reduced norepinephrine in histologically normal myocardium adjacent to transmural infarction in the cat. The relation between reduced sympathetic innervation and mechanical function has not been previously examined.

Minardo et al. (19) used I-123 MIBG to show that the area of denervation extended beyond the region of infarction and demonstrated supersensitivity of refractory period shortening to adrenergic stimulation by norepinephrine. Dae et al. (20) found denervation in tissue adjacent and distal to transmural infarction in a canine model on day 6 after infarction by I-123 MIBG scintigraphy, reduced norepinephrine content and nerve fluorescence. These investigators also demonstrated that

nontransmural infarction is associated with preservation of sympathetic innervation in the adjacent zone.

McGhie et al. (21) evaluated 27 patients on day 10 after acute MI with I-123 MIBG scintigraphy in border and distant zones and found reduced uptake and a more extensive area of reduced uptake than the thallium perfusion defect. These regions are associated with spontaneous ventricular tachyarrhythmias in humans after MI (22).

Sympathetic reinnervation after infarction. Reinnervation at later time points after infarction in peri-infarct regions has been demonstrated by return of MIBG scintigraphic images to normal by 14 weeks after infarction (19). The process of reinnervation is likely incremental, in that Nishimura et al. (23) demonstrated steady recovery of tissue norepinephrine content in peri-infarct regions between the first and sixth week after infarction in a canine model. We previously showed in the same animal model some improvement in function in adjacent noninfarcted regions between 1 and 8 weeks after infarction (1). Reinnervation may be in part responsible for the return of function during this period.

Reinnervation may be incomplete, however, as late as 3 months after MI, as shown by Hartikainen et al. (24). These investigators examined I-123 MIBG uptake in humans at 3 and 12 months after a first MI and found no difference in MIBG activity over time within the infarct zone, but an increase in activity in the peri-infarcted region without a change in perfusion as measured by technetium-99m sestamibi scintigraphy. The size of the peri-infarct zone, as defined by reduced MIBG uptake but normal perfusion, did not change over this period. The border regions also demonstrated recovery of metabolic activity as measured by I-123 paraphenylpentadecanoic acid in association with reinnervation. However, we have previously demonstrated no further improvement in function in adjacent noninfarcted regions beyond 8 weeks after MI, specifically between 8 weeks and 6 months after infarction (1).

Study limitations. The 1-h period after MIBG infusion before excision of the heart might be short in that some investigators have demonstrated a low affinity, nonneuronal MIBG uptake mechanism in the heart (7,25,26). However, Rabinovitch et al. (27) have shown that there is a very rapid blood clearance in the first 30 min after infusion, suggesting that blood content could not explain differences in MIBG uptake. Most of the early MIBG accumulation is in the liver and vesicles of peripheral sympathetic nerves (27).

Some investigators have suggested (22) that there is a normal apex to base gradient in myocardial norepinephrine, with apical stores being lower. Apical thinning on tomographic imaging may account for this in part. If this is so, adjacent regions that are apical to remote regions could demonstrate reduced MIBG uptake on that basis alone. However, in the noninfarcted control animals studied, quantitative MIBG uptake was not different in the apex relative to the base.

Analysis of sympathetic innervation involves presynaptic sympathetic function and does not address changes in postsynaptic function. Regional alterations in beta-adrenergic receptor density and function (28) might impact significantly on the remodeling process.

Only one time point during the period of LV remodeling after infarction was studied. The interaction between reinnervation and changes in regional function over the 8-week period was not studied. We previously showed (1) that adjacent noninfarcted region function does not change significantly between 8 weeks and 6 months after MI, suggesting that any reinnervation that occurs after 8 weeks may not influence regional function.

Finally, it is unlikely that all of the dysfunction in adjacent noninfarcted regions is explained by reduced sympathetic innervation. One reason is that the relative magnitude of dysfunction tended to be greater than that of denervation in adjacent noninfarcted regions. In addition, other mechanisms may be at work, including increased local wall stress and altered postsynaptic adrenergic function.

Potential clinical implications. Sympathetic denervation may contribute to dysfunction seen in noninfarcted regions in human infarction (29). Through its interplay with sympathetic innervation, pharmacologic therapy after MI (e.g., beta-blockade) might modulate regional function. MIBG scintigraphy in the postinfarct patient, in combination with imaging of LV function, could improve our understanding of the in vivo relation of sympathetic innervation to changes in regional intramyocardial function.

We gratefully acknowledge the support of the surgical research staff of Allegheny University of the Health Sciences, Pittsburgh campus, including Leslie DeFranc, Melissa Krukenberg, Maureen Miller and Stephen Cherilla, and the nuclear cardiology and magnetic resonance technologists at Allegheny General Hospital, especially Anthony Petraglia, June Yamrozik and Lois Miller.

References

1. Kramer CM, Lima JAC, Reichek N, et al. Regional function within noninfarcted myocardium during left ventricular remodeling. Circulation 1993;88:1279–88.
2. Melillo G, Lima JAC, Judd RM, Goldschmidt-Clermont PJ, Silverman HS. Intrinsic myocyte dysfunction and tyrosine kinase pathway activation underlie the impaired wall thickening of adjacent regions during postinfarct left ventricular remodeling. Circulation 1996;93:1447–58.
3. Mitchell GF, Lamas GA, Vaughan DE, Pfeffer MA. Left ventricular remodeling in the year after first anterior myocardial infarction. J Am Coll Cardiol 1992;19:1136–44.
4. Barber MJ, Mueller TM, Henry DP, Felten SY, Zipes DP. Transmural myocardial infarction in the dog produces sympathectomy in noninfarcted myocardium. Circulation 1983;67:787–95.
5. Uren NG, Crake T, Lefroy D, de Silva R, Davies G, Maseri A. Reduced coronary vasodilator function in infarcted and normal myocardium after myocardial infarction. N Engl J Med 1994;331:222–7.
6. Olivetti G, Capasso JM, Meggs LG, Sonnenblick EH, Anversa P. Cellular basis of chronic ventricular remodeling after myocardial infarction in rats. Circ Res 1991;68:856–69.
7. Wieland DM, Brown LE, Rogers WI, et al. Myocardial imaging with a radioiodinated norepinephrine storage analog. J Nucl Med 1981;22:22–31.
8. Tobes MC, Jaques S Jr., Wieland DM, Sisson JC. Effect of uptake-one inhibitors on the uptake of norepinephrine and meta-iodobenzylguanidine. J Nucl Med 1985;26:897–907.
9. Dae MW, O'Connell JW, Botvinick EH, et al. Scintigraphic assessment of regional cardiac adrenergic innervation. Circulation 1989;79:634–44.
10. Zerhouni E, Parrish D, Rogers WJ, Yang A, Shapiro EP. Human heart:

tagging with MR imaging—a method for noninvasive measurement of myocardial motion. Radiology 1988;169:59–64.
11. Axel L, Dougherty L. MR imaging of motion with spatial modulation of magnetization. Radiology 1989;171:841–5.
12. Clark N, Reichek N, Bergey P, et al. Normal segmental myocardial function: assessment by magnetic resonance imaging using spatial modulation of magnetization. Circulation 1991;84:67–74.
13. Glenny RW, Bernard S, Brinkley M. Validation of fluorescent-labeled microspheres for measurement of regional organ perfusion. J Appl Physiol 1993;74:2585–97.
14. Markovitz LJ, Savage EB, Ratcliffe MB, et al. Large animal model of left ventricular aneurysm. Ann Thorac Surg 1989;48:838–45.
15. McVeigh ER, Atalar E. Cardiac tagging with breath-hold cine MRI. Magn Res Med 1992;28:318–27.
16. Kramer CM, Ferrari VA, Rogers WJ, et al. ACE inhibition limits dysfunction in adjacent noninfarcted regions during left ventricular remodeling. J Am Coll Cardiol 1996;27:211–7.
17. Washburn LC, Khosla RC, Williams CC, Gelfand MJ, Maxon HR. Production and application of I^{123}-labeled M-iodobenzylguanidine. In: Emran AM, editor. Chemists' Views of Imaging Centers. New York: Plenum Press, 1995:291–8.
18. Kozlovskis PL, Fieber LA, Bassett AL, Cameron JS, Kimura S, Myerburg RJ. Regional reduction in ventricular norepinephrine after healing of experimental myocardial infarction in cats. J Mol Cell Cardiol 1986;18:413–22.
19. Minardo JD, Tuli MM, Mock BH, et al. Scintigraphic and electrophysiological evidence of canine myocardial sympathetic denervation and reinnervation produced by myocardial infarction or phenol application. Circulation 1988;78:1008–19.
20. Dae MW, Herre JM, O'Connell JW, Botvinick EH, Newman D, Munoz L. Scintigraphic assessment of sympathetic innervation after transmural versus nontransmural myocardial infarction. J Am Coll Cardiol 1991;17:1416–23.
21. McGhie AI, Corbett JR, Akers MS, et al. Regional cardiac adrenergic function using I^{123}meta-iodobenzylguanidine tomographic imaging after acute myocardial infarction. Am J Cardiol 1991;67:236–42.
22. Stanton MS, Tuli MM, Radtke NL, et al. Regional sympathetic denervation after myocardial infarction in humans detected noninvasively using I^{123}metaiodobenzylguanidine. J Am Coll Cardiol 1989;14:1519–26.
23. Nishimura T, Oka H, Sago M, et al. Serial assessment of denervated but viable myocardium following acute myocardial infarction in dogs using iodine-123 metaiodobenzylguanidine and thallium-201 chloride myocardial single photon emission tomography. Eur J Nucl Med 1992;19:25–9.
24. Hartikainen J, Kuikka J, Mantysaari M, Lansimies E, Pyorala K. Sympathetic reinnervation after acute myocardial infarction. Am J Cardiol 1996; 77:5–9.
25. Sisson JC, Wieland DM, Sheman P, et al. Metaiodobenzylguanidine to map scintigraphically the adrenergic nervous system in man. J Nucl Med 1987; 28:1625–36.
26. Nakajo M, Shimabukuro K, Yoshimura H, et al. Iodine-131–meta-iodobenzylguanidine intra- and extravesicular accumulation in the rat heart. J Nucl Med 1986;27:84–9.
27. Rabinovitch MA, Rose CP, Schwab AJ, et al. A method of dynamic analysis of iodine-123–metaiodobenzylguanidine scintigrams in cardiac mechanical overload hypertrophy and failure. J Nucl Med 1993;34:589–600.
28. Kozlovskis PL, Smets MJD, Duncan RC, Bailey BK, Bassett AL, Myerburg RJ. Regional beta-adrenergic receptors and adenylate cyclase activity after healing of myocardial infarction in cats. J Mol Cell Cardiol 1990;22:311–22.
29. Kramer CM, Rogers WJ, Theobald T, Power TP, Petruolo S, Reichek N. Remote noninfarcted region dysfunction soon after first anterior myocardial infarction: a magnetic resonance tagging study. Circulation 1996;94:660–6.